Transition to turbulence in hypersonic flow

By J. J. W. van der Vegt

An outline of the project and recent progress toward the study of transition in hypersonic boundary layers is given. Aspects of the numerical method and the results of test computations are presented. At present the laminar flows over a flat plate and wedge have been computed for $M \leq 5$.

1. Motivation and objective

The prediction of transition to turbulence is of crucial importance in the design of space vehicles currently planned, such as the trans-atmospheric vehicle (TAV) and the aeroassisted transfer vehicle (AOTV). The state of the boundary layer, laminar or turbulent, has a dramatic influence on the heating of the surface and drag. Surface heating poses a bigger threat for this type of vehicles than previous ones because they do not have spherical noses and ablative heat shields. The main tools presently available for predicting transition in hypersonic flow are experiments and e^N -stability theory. Both are of great importance in the design of space vehicles, but they also suffer serious deficiencies. A serious problem with wind-tunnel experiments is noise, which causes earlier transition than in free flight. New results in the quiet Mach 3.5 pilot wind-tunnel at NASA Langley show a dramatic difference in transition compared with older, noisier tunnels, (Chen et al. 1989). Another serious problem with wind-tunnel experiments is that it is impossible to scale the chemistry effects properly. These effects are important at hypersonic speeds where the temperatures are so high that real gas effects and chemical changes become important. Therefore, in addition to wind-tunnel experiments, free flight experiments and theoretical tools are indispensable.

Among the theoretical tools, e^N-stability theory, which uses linear stability theory together with an experimentally determined N-factor, is by far the most widely used. Originally an incompressible flow method, it has been extended to compressible flow by Mack (for a review see Mack, 1984), and applied to hypersonic flow by Malik (1989) and Gasperas (1987-89). The method has as its main advantage that, for low disturbance levels and approximately parallel mean flow, it generally gives reasonable answers when accompanied with a suitable N-factor obtained by experiments. Using new results from the quiet Mach 3.5 wind-tunnel, Chen et al. (1989) showed that linear stability results compare more favorably with experiments on a cone than previous results. There are, however, problems in using linear stability theory. For instance, it cannot predict the effects of a shock on transition, which can be important in certain applications. It also fails when non-linear effects are important. Compared to incompressible flow, however, non-linear stability theories for hypersonic flow are still in their infancy and much remains to be accomplished.

The purpose of this research is to provide additional information about transition to turbulence in hypersonic flow by using direct numerical simulation of hypersonic flows, together with non-linear stability theory. Special attention is paid to the interaction between a shock and a boundary layer, in the so-called shock layer. The two cases which will be investigated in more detail are a flat plate boundary layer and the flow about a wedge. The flat plate boundary layer is studied because it gives an opportunity to compare results with linear stability theory. The second case, the flow about a wedge, offers the opportunity to study the effects of extreme heating and shocks on transition in the shock layer.

2. Accomplishments

The main activity in 1989 has been the development of a numerical method for the solution of the compressible Navier-Stokes equations and writing and testing a computer program based on this method. In the next section the numerical method will be discussed and motivation for the choices made will be given. Results of test computations will be presented in the subsequent section.

3. Numerical method

Although the main objective of this project is to study hypersonic transition, it was decided to follow a stepwise approach to code development and test each component separately. In the design of the program and the choice of numerical method, however, the ultimate goal, hypersonic flow, was kept in mind, so the code is not necessarily optimal for intermediate problems. For instance, the program can handle an arbitrary equation of state, while in memory management extensions to larger sets of equations are anticipated.

The code must both give accurate steady state solutions with a reasonable efficiency and allow time accurate solutions. These are conflicting requirements, because for the steady case one can obtain fast convergence by adding dissipation, while one tries to minimize dissipation in time accurate calculations. Whenever there is a conflict between these requirements, time accuracy was favoured. The flow field contains both strong shocks and boundary layers, which present different problems. The addition of real gas chemistry makes the problem very stiff and puts strong limits on the time step for an explicit method, making the use of an implicit method almost mandatory. For time accurate implicit calculations, the time step cannot be too large, if all the time scales of fluid motion are to be resolved, while the faster chemical time scales are ignored by using an implicit method.

An implicit method is much more complicated than an explicit method. There are a number of implicit methods available for the compressible Navier-Stokes equations. One of the first and most widely used methods is that of Beam and

Warming (1978), which is not well suited for our problem. For time accurate solutions the approximate factorization used in the Beam and Warming algorithm adds an additional error and the viscous cross-coupling terms cannot be taken into account implicitly. In addition the method requires artificial viscosity to obtain stable solutions when there are shocks, due to the use of central differences. The Beam-Warming method is designed for obtaining steady state solutions efficiently, but is not well suited to time accurate calculations.

An alternative is a method based on splitting the non-linear terms in the Navier-Stokes equations into components related to the positive and negative eigenvalues of the operator. The method accounts for the traveling of information along the (inviscid) characteristics in the differencing. Although the flow is viscous, due to the high Reynolds number, this is not a bad approximation in most areas of the flow. Recently Montagné et al. (1989) compared various algorithms, such as flux splitting according to Steger and Warming or van Leer, approximate Riemann solvers and TVD methods for real gas equations and did not find major differences in their prediction of shock waves. Because we cannot hope to resolve the details of a shock in our simulation, we are forced to use one of these methods or central differencing with additional artificial dissipation. The choice was made to use flux splitting for the non-linear terms for its additional beneficial numerical effects, viz. a diagonally dominant matrix suited for an iterative method. In the viscous region, however, one has to be careful, because flux splitting can produce unwanted numerical dissipation, as was demonstrated by MacCormack et al. (1989). The correction to the Steger-Warming splitting proposed by MacCormack is used in regions with dominant viscous effects, whereas in a shock the Steger-Warming splitting, as described in Steger et al. (1981), is used. The fact that the flux splitting of the non-linear terms, accompanied by one sided differencing, results in a diagonally dominant matrix, which can be solved iteratively, was used to incorporate all the viscous components implicitly in the numerical method. This was impossible in the factored algorithm of Beam and Warming. It also gives more freedom in the choice of boundary conditions.

The numerical technique chosen to discretize the equations is a finite volume method because an integral formulation is better suited to flows with shocks, and it always satisfies the conservation properties of the equations. The present algorithm solves the two-dimensional compressible Navier-Stokes equations in conservation form in an arbitrary coordinate system. These can be written as:

$$\frac{\partial}{\partial t}\hat{\mathbf{U}} + \frac{\partial}{\partial \xi}(\hat{\mathbf{E}} - \hat{\mathbf{V}}_{vis_\xi}) + \frac{\partial}{\partial \eta}(\hat{\mathbf{G}} - \hat{\mathbf{V}}_{vis_\eta}) = \mathbf{0}$$

with:

$$\hat{\mathbf{U}} = \frac{\mathbf{U}}{J}; \quad \hat{\mathbf{E}} = \frac{\xi_x}{J}\mathbf{E} + \frac{\xi_z}{J}\mathbf{G}; \quad ,\hat{\mathbf{G}} = \frac{\eta_x}{J}\mathbf{E} + \frac{\eta_z}{J}\mathbf{G} \tag{1}$$

$$\hat{\mathbf{V}}_{vis_\xi} = \frac{\xi_x}{J}\mathbf{V} + \frac{\xi_z}{J}\mathbf{I}; \quad \hat{\mathbf{V}}_{vis_\eta} = \frac{\eta_x}{J}\mathbf{V} + \frac{\eta_z}{J}\mathbf{I} \tag{2}$$

and:

$$\mathbf{U} = \begin{pmatrix} \rho \\ \rho u \\ \rho w \\ e \end{pmatrix}; \quad \mathbf{E} = \begin{pmatrix} \rho u \\ \rho u^2 + p \\ \rho u w \\ (e+p)u \end{pmatrix}; \quad \mathbf{G} = \begin{pmatrix} \rho w \\ \rho u w \\ \rho w^2 + p \\ (e+p)w \end{pmatrix} \tag{3}$$

$$\mathbf{V} = \frac{1}{Re}\begin{pmatrix} 0 \\ \tau_{xx} \\ \tau_{xz} \\ u\tau_{xx} + w\tau_{xz} - \frac{q_x}{(\gamma-1)M^2 Pr} \end{pmatrix}; \quad \mathbf{I} = \frac{1}{Re}\begin{pmatrix} 0 \\ \tau_{xz} \\ \tau_{zz} \\ u\tau_{xz} + w\tau_{zz} - \frac{q_z}{(\gamma-1)M^2 Pr} \end{pmatrix} \tag{4}$$

$$\tau_{xx} = (2\mu+\lambda)\frac{\partial u}{\partial x} + \lambda\frac{\partial w}{\partial z}; \quad \tau_{xz} = \mu(\frac{\partial u}{\partial z} + \frac{\partial w}{\partial x}); \quad \tau_{zz} = (2\mu+\lambda)\frac{\partial w}{\partial z} + \lambda\frac{\partial u}{\partial x} \tag{5}$$

$$q_x = -\kappa\frac{\partial T}{\partial x}; \quad q_z = -\kappa\frac{\partial T}{\partial z} \tag{6}$$

together with the equation of state: $p = \frac{\rho c_v T}{\gamma M^2}$

Here ρ represents the density, u and v the velocity components in a Cartesian coordinate system, p the pressure, T temperature and e the total energy. The variables x and y represent the Cartesian coordinates, whereas ξ and η represent curvilinear coordinates. The coefficients M and Pr are the Mach and Prandtl numbers, whereas μ, λ and κ are the two viscosities and the thermal conductivity respectively. It is important to realize that the shear stress and heat flux components in **V** and **I** are functions of ξ and η. The equations are solved in a general coordinate system because the wedge does not allow an orthogonal coordinate system and complicated local flow phenomena, such as shocks, and boundary layers require local grid refinement. The use of generalized coordinates, however, greatly increases the complexity of the code.

The basic steps in the development of the numerical scheme will now be summarized. The first step is the choice of a time integration method. The time integration is formulated as a Padé relation, cf. Beam and Warming (1978):

$$\triangle\hat{\mathbf{U}}^n = \frac{\alpha\triangle t}{1+\beta}\frac{\partial}{\partial t}\triangle\hat{\mathbf{U}}^n + \frac{\triangle t}{1+\beta}\frac{\partial}{\partial t}\hat{\mathbf{U}}^n + \frac{\beta}{1+\beta}\hat{\mathbf{U}}^{n-1} + O[(\alpha-\frac{1}{2}-\beta)\triangle t^2 + \triangle t^3] \quad (7)$$

with: $\triangle\hat{\mathbf{U}}^n = \hat{\mathbf{U}}^{n+1} - \hat{\mathbf{U}}^n$

Here the coefficients α and β allow different time integration schemes to be obtained. For instance, $\alpha = 1$, $\beta = 0$, give the implicit Euler method, $\alpha = .5$, $\beta = 0$ give the trapezium rule and $\alpha = 1$, $\beta = 0.5$ give a three point backward scheme. The superscript n in this equation refers to the time $t = t_n$.

Introducing the compressible Navier-Stokes equations (1) into this relation yields:

$$\begin{aligned}\triangle\hat{\mathbf{U}}^n = &\frac{\alpha\triangle t}{1+\beta}\{-\frac{\partial}{\partial\xi}(\triangle\hat{\mathbf{E}}^n - \triangle\hat{\mathbf{V}}^n_{vis_\xi}) - \frac{\partial}{\partial\eta}(\triangle\hat{\mathbf{G}}^n - \triangle\hat{\mathbf{V}}^n_{vis_\eta})\} + \\ &\frac{\triangle t}{1+\beta}\{-\frac{\partial}{\partial\xi}(\hat{\mathbf{E}}^n - \hat{\mathbf{V}}^n_{vis_\xi}) - \frac{\partial}{\partial\eta}(\hat{\mathbf{G}}^n - \hat{\mathbf{V}}^n_{vis_\eta})\} + \frac{\beta}{1+\beta}\hat{\mathbf{U}}^{n-1}\end{aligned} \quad (8)$$

which is first or second order accurate in time, depending on the choice of α and β. In order to solve this set of non-linear equations for the implicit case, the flux vectors must be linearized around their value at time $t = t_n$:

$$\triangle\hat{\mathbf{E}}^n(\mathbf{U}) \cong \left(\frac{\partial\hat{\mathbf{E}}^n}{\partial\mathbf{U}}\right)_+ \triangle\mathbf{U}^n + \left(\frac{\partial\hat{\mathbf{E}}^n}{\partial\mathbf{U}}\right)_- \triangle\mathbf{U}^n \quad (9)$$

$$\triangle\hat{\mathbf{V}}^n_{vis_\xi}(\mathbf{U}) \cong \frac{\partial\hat{\mathbf{V}}^n_{vis_\xi}}{\partial\mathbf{U}}\triangle\mathbf{U}^n + \frac{\partial\hat{\mathbf{V}}^n_{vis_\xi}}{\partial\mathbf{U}_\xi}\triangle\mathbf{U}^n_\xi + \frac{\partial\hat{\mathbf{V}}^n_{vis_\xi}}{\partial\mathbf{U}_\eta}\triangle\mathbf{U}^n_\eta \quad (10)$$

with similar linearizations for the vectors $\triangle\mathbf{G}^n$ and $\triangle\hat{\mathbf{V}}^n_{vis_\eta}$. The suffices + and − on the Jacobian matrices of the inviscid flux vectors refer to the components with positive and negative eigenvalues. Introducing the linearizations of the flux vectors in (8) and integrating over a small volume gives the integral formulation for the compressible Navier-Stokes equations:

$$\frac{1}{V_{ij}}\int\limits_{V_{ij}}\frac{1}{J}\triangle\mathbf{U}^n dV+\frac{\alpha\triangle t}{1+\beta}\frac{1}{V_{ij}}\int\limits_{S_{ij}}\{n_\xi\Big(\Big(\left(\frac{\partial\hat{\mathbf{E}}^n}{\partial\mathbf{U}}\right)_+ +\left(\frac{\partial\hat{\mathbf{E}}^n}{\partial\mathbf{U}}\right)_- -\frac{\partial\hat{\mathbf{V}}^n_{vis_\xi}}{\partial\mathbf{U}}\Big)\triangle\mathbf{U}^n-$$

$$\frac{\partial\hat{\mathbf{V}}^n_{vis_\xi}}{\partial\mathbf{U}_\xi}\triangle\mathbf{U}^n_\xi-\frac{\partial\hat{\mathbf{V}}^n_{vis_\xi}}{\partial\mathbf{U}_\eta}\triangle\mathbf{U}^n_\eta\Big)+n_\eta\Big(\Big(\left(\frac{\partial\hat{\mathbf{G}}^n}{\partial\mathbf{U}}\right)_+ +\left(\frac{\partial\hat{\mathbf{G}}^n}{\partial\mathbf{U}}\right)_- -\frac{\partial\hat{\mathbf{V}}^n_{vis_\eta}}{\partial\mathbf{U}}\Big)\triangle\mathbf{U}^n-$$

$$\frac{\hat{\mathbf{V}}^n_{vis_\eta}}{\partial\mathbf{U}_\xi}\triangle\mathbf{U}^n_\xi-\frac{\hat{\mathbf{V}}^n_{vis_\eta}}{\partial\mathbf{U}_\eta}\triangle\mathbf{U}^n_\eta\Big)\}dS=$$

$$-\frac{\triangle t}{1+\beta}\frac{1}{V_{ij}}\int\limits_{S_{ij}}\{n_\xi\Big(\Big(\left(\frac{\partial\hat{\mathbf{E}}^n}{\partial\mathbf{U}}\right)_+ +\left(\frac{\partial\hat{\mathbf{E}}^n}{\partial\mathbf{U}}\right)_-\Big)\mathbf{U}^n-\hat{\mathbf{V}}^n_{vis_\xi}\Big)+n_\eta\Big(\Big(\left(\frac{\partial\hat{\mathbf{G}}^n}{\partial\mathbf{U}}\right)_+ +$$

$$\left(\frac{\partial\hat{\mathbf{G}}^n}{\partial\mathbf{U}}\right)_-\Big)\mathbf{U}^n-\hat{\mathbf{V}}^n_{vis_\eta}\Big)\}dS+\frac{\beta}{1+\beta}\frac{1}{V_{ij}}\int\limits_{V_{ij}}\frac{1}{J}\hat{\mathbf{U}}^{n-1}dV \tag{11}$$

Here V_{ij} represents a grid cell, S_{ij} a cell surface and n_ξ and n_η outward normal vectors at S_{ij}. The final step consists of approximating the fluxes across the cell surfaces S_{ij}. The positive and negative flux vectors are differenced backward and forward respectively, while the viscous terms are centrally differenced. In boundary layer regions the modifications to the differencing of the inviscid flux vectors presented by MacCormack et al. (1989) are used, whereas in a shock the Steger-Warming splitting is used, see Steger et al.(1981). After choosing proper discretizations for the components at the cell surfaces and centers, a system of linear algebraic equations is obtained:

$$\hat{A}^n_{ij}\triangle\mathbf{U}^n_{i,j}+\hat{B}^n_{ij}\triangle\mathbf{U}^n_{i,j+1}+\hat{C}^n_{ij}\triangle\mathbf{U}^n_{i,j-1}+\hat{D}^n_{ij}\triangle\mathbf{U}^n_{i+1,j}+\hat{E}^n_{ij}\triangle\mathbf{U}^n_{i-1,j}+$$

$$\hat{F}^n_{ij}\triangle\mathbf{U}^n_{i+1,j+1}+\hat{G}^n_{ij}\triangle\mathbf{U}^n_{i-1,j+1}+\hat{H}^n_{ij}\triangle\mathbf{U}^n_{i+1,j-1}+\hat{I}^n_{ij}\triangle\mathbf{U}^n_{i-1,j-1}=\hat{\mathbf{R}}^n_{ij}$$

Here $\hat{A}^n_{ij},\cdots,\hat{I}^n_{ij}$ represent the Jacobian matrices obtained after linearization of the flux vectors and $\mathbf{R}^n_{ij}$ is the right-hand side. For the compressible Navier-Stokes equations they are 4×4 matrices, but for real gases they are much larger. The details of these matrices will be published elsewhere.

The solution of this system is the most time consuming part of the numerical algorithm. The use of flux splitting for the non-linear terms makes the matrices diagonally dominant and allows the use of iterative methods. Gauss-Seidel line relaxation is used in all four directions of the fluid domain to reduce the nona-diagonal block matrix to a tri-diagonal matrix. This system of tri-diagonal matrices is usually solved with a direct inversion method because these matrices do not have a structure suitable for most iterative inversion methods. If the mean flow quantities are needed, it is not necessary to iterate this Gauss-Seidel line relaxation to convergence at each time step, but for time accurate solutions convergence to accuracy better than the truncation error must be obtained each time step. The inversion may become then prohibitively expensive. So an alternative to the direct inversion must be found. It was suggested by Dexun et al. (1989) that using the LU decomposition of the abridged matrices, consisting of only the main diagonals of the tri-diagonal block matrices, as a preconditioner and solving the tri-diagonal block matrices iteratively gives a significant improvement in computational efficiency. It is convergent for time steps very close to the maximum allowable ones of the total scheme. The fully iterative scheme so obtained converges very rapidly. In two to four Gauss-Seidel sweeps machine accuracy is obtained. The inner iteration, used to solve the block tri-diagonal matrices in each Gauss-Seidel sweep, converges in about ten to fifteen iterations for the first Gauss-Seidel sweep and in one to four the following inner iterations, thereby greatly reducing the computational time. Further tests to improve convergence by using residual correction and under- or over-relaxation did not improve the convergence rate. The improvements in the solution of the system of linear equations will be of great importance when the full real gas equations are solved because the blocks in the nona-diagonal matrix are much larger.

The outflow boundary conditions are zeroth order extrapolation, which performed well and had no noticeable upstream influence. This condition is, however, not suitable for direct simulations because of its reflective properties. The main source of trouble at the outflow boundary is the subsonic region close to the wall. The technique of setting the pressure in this region to the free-stream pressure does not work because it creates instabilities whenever the pressure becomes smaller than the free-stream pressure. The boundary conditions at the solid surface also require special attention. The set of boundary conditions used for an adiabatic wall consisted of zero velocity and heat flux at the wall, determining the pressure from the equation of state and using the continuity and energy equations to close the system. The conditions are implemented using a half cell at the solid wall, as discussed in Vinokur (1989), and works very well. Conditions such as zero normal pressure gradient and/or zero density gradient are not valid at the wall in a viscous fluid and should not be used.

4. Test results

Careful testing has been performed to investigate the accuracy of the numerical scheme and seek errors in the code. After preliminary test cases, such as uniform flow and a normal shock, the main test case was to compare the results of the computations of the flow about an adiabatic flat plate at zero angle of incidence with the analytically derived results from Crocco (1941), see also Schlichting (1979). In order to test the ability of the model to compute shocks, the case of a finite plate in a uniform flow was considered and the results at the trailing edge were compared with the boundary layer results of Crocco. This also removed the problem of choosing an inflow profile. Due to the fact that at the nose of the plate both the x- and y-derivatives are equally important, it is necessary to use small square grid cells in this region, see Fig. 1, while strong grid stretching is required in the boundary layer region. If the grid is stretched too much in one direction at the nose, divergence of the computations results. The general features of the flow field are presented in Fig. 2, which shows the pressure field at steady state for Mach number 2. The plot shows a large pressure jump at the nose of the plate, followed by an expansion around the outer edge of the boundary layer, while a weak shock originates from the nose of the plate. After the nose region the flow relaxes to a boundary layer. The temperature and velocity in the region just ahead of the trailing edge are compared with the theoretical results of Crocco. In Fig. 3 and 4 the Steger-Warming splitting and MacCormack splitting on a 42×42 grid are compared with the results of Crocco, and it is clear that the Mc Cormack splitting gives much better results; the Steger-Warming splitting is much too dissipative in the boundary layer. The results close to the wall are not bad, because this region has most of the gridpoints. It must be remarked, however, that the Steger-Warming splitting does not perform as badly as claimed by MacCormack et al. (1989). To give, however, a more definite answer about the accuracy the effects of grid refinement have to be investigated, this is currently being done.

A problem in the calculations is to define an initial field. The computations for $M = 2$ were started from a uniform flow field, but in the computations at higher Mach numbers, the Mach 2 result was used as initial field.

For all these cases, the iterative matrix inversion works without problems and is convergent for a time step very close to the stability limit of the scheme. Due to the presence of a shock and the reduction of numerical viscosity, the time step for the calculations was, however, rather restricted. This is no surprise because an analysis of implicit schemes for Burger's equation, done by Poinsot et al. (1985), shows the same result. Further tests are currently being performed on the calculation of the viscous flow about a wedge.

5. Work to be done:

• Testing the code for time accuracy. This will be done using the most unstable mode from linear stability theory and comparing growth rates. Propagation of sound waves is another interesting test case.

• Improvement of inflow and outflow boundary conditions for time accurate solutions, so that they are non-reflecting and compatible with Navier-Stokes equations.

• The results of the first two steps may show that the spatial order of the difference scheme must be increased.

• Study of transition in supersonic flow. This will be done by introducing small disturbances into the flow. It will be accompanied by the development of non-linear stability theory. Without a more advanced stability theory, it will be difficult to do a complete study of transition phenomena, due to the many parameters involved and the extremely long computation times of the simulations. Stability theory is, however, still in its infancy and will require a significant effort. Preliminary investigations show that the non-linear geometrical optics used by Artola and Majda (1989) is a good starting point.

The specific cases which will be investigated are:

Shock layer: For this case a wedge connected to a flat plate, compression corner will be used. The effects of the shock on the boundary layer can be investigated systematically as a function of wedge angle and Mach and Reynolds number.

Free stream disturbances: An important reason for inaccuracies in linear stability theory are the effects of free stream disturbances. The effects of small amplitude sound waves and free stream vorticity on the boundary layer on a cone will be studied and compared with the experiments of Chen et al. 1989, which show the effects of sound waves on transition. An important issue in this case is resonance between reflected and transmitted waves at the shock and the influence of the body. These effects on a vortex layer are also studied in Artola and Majda (1989) using non-linear geometrical optics and application of their theory to the flow on a cone or wedge will be very useful.

• Adding real gas effects to the code. This is a major, but rather straightforward extension of the program and allows the study of real gas effects on transition.

REFERENCES

ARTOLA, M. & MAJDA, A. J. 1989 Nonlinear Development of Instabilities in Supersonic Vortex Sheets II: Resonant Interaction Among Kink Modes. *SIAM Journal of Applied Mathematics.* **49**, 1310-1349.

BEAM, R. M. & WARMING, R. F. 1978 An Implicit Factored Scheme for the Compressible Navier-Stokes Equations. *AIAA Journal.* **16**, No 4, 393-402.

CHEN, F. J., MALIK, M. R. & BECKWITH, I. E. 1989 Boundary-Layer Transition on a Cone and Flat Plate at Mach 3.5. *AIAA Journal.* **27**, No. 6, 687-693.

CROCCO, L. 1941 Sullo Strato Limite Laminare Nei Gas Lungo Una Lamina Piana, Rendiconti di Matematica delle sue Applicazioni, University Rome, 139-152.

DEXUN, F. & YANWEN, M. 1989 On Efficiency and Accuracy of Numerical Methods for Solving Aerodynamic Equations, Symposium Tokyo.

GASPERAS, G. 1987 The Stability of the Compressible Boundary Layer on a Sharp Cone at Zero Angle of Attack, AIAA Conference Reno, paper AIAA-87-0494.

GASPERAS, G. 1989 Transition Prediction for Two-Dimensional Viscous Supersonic Wakes, AIAA Conference Reno, paper AIAA-89-0284.

MACCORMACK, R. W. & CANDLER, G. V. 1989 The Solution of the Navier-Stokes Equations using Gauss-Seidel Line Relaxation. *Computers and Fluids.* **17**, 135-150.

MACK, L. M. 1984 Boundary-Layer Linear Stability Theory, Special Course on Stability and Transition of Laminar Flow, AGARD Report, No. 709.

MALIK, M. R. 1989 Transition in Hypersonic Boundary Layers, AIAA Conference Reno, 1989.

MONTAGNÉ, J. L., YEE, H., C. & VINOKUR, M. 1989 Comparative Study of High-Resolution Shock-Capturing Schemes for a Real Gas. *AIAA Journal.* **27**, No.10, 1332-1346.

POINSOT, T. & CANDEL, S. M. 1986 The Influence of Differencing and CFL Number on Implicit Time-Dependent Non-Linear Calculations. *Journal of Computational Physics.* **62**, 282-296.

SCHLICHTING, H. 1979 Boundary Layer Theory, Mc Graw-Hill.

STEGER, J. L. & WARMING, R. F. 1981 Flux-Vector Splitting of the Inviscid Gasdynamic Equations with Application to Finite Difference Methods. *Journal of Computational Physics.* **40**, 263-293.

VINOKUR, M. 1989 An Analysis of Finite-Difference and Finite-Volume Formulations of Conservation Laws. *Journal of Computational Physics.* **81**, 1-52.

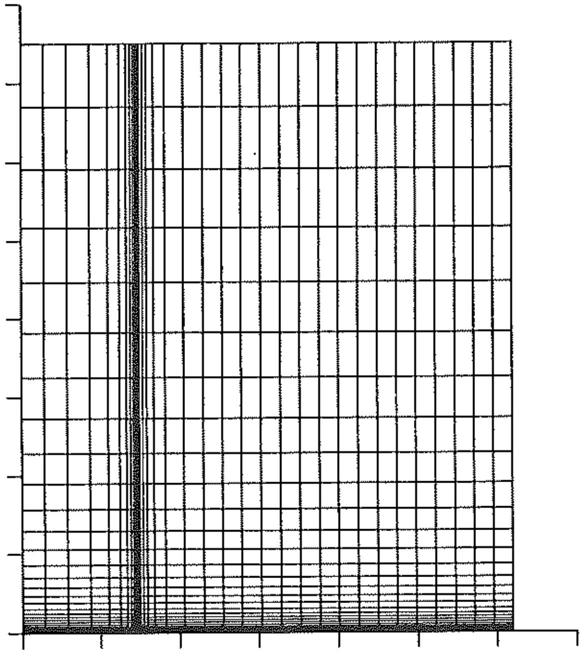

FIGURE 1. Grid for calculation of flow field above flat plate.

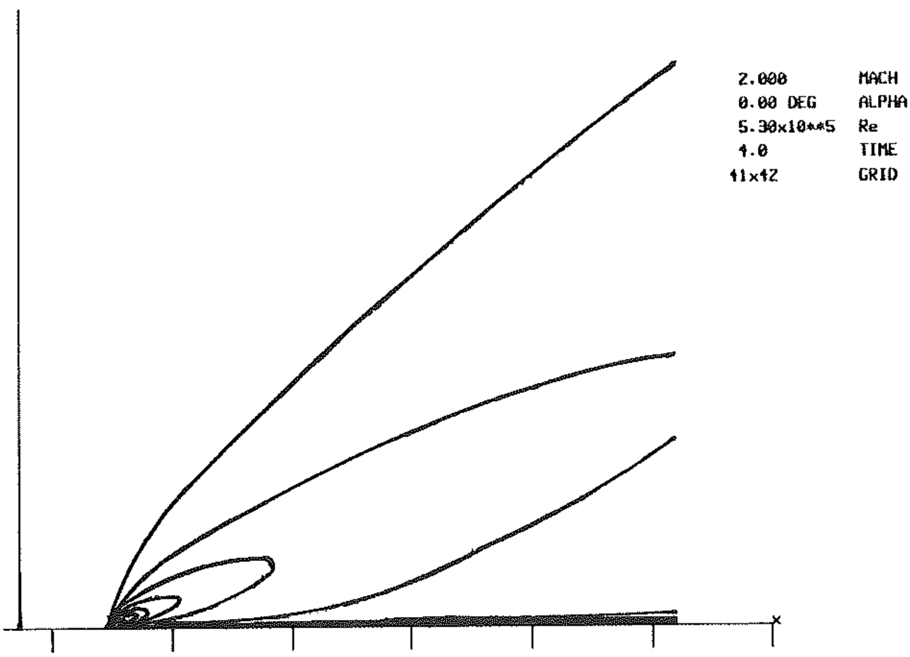

FIGURE 2. Pressure field above flat plate at Mach = 2.

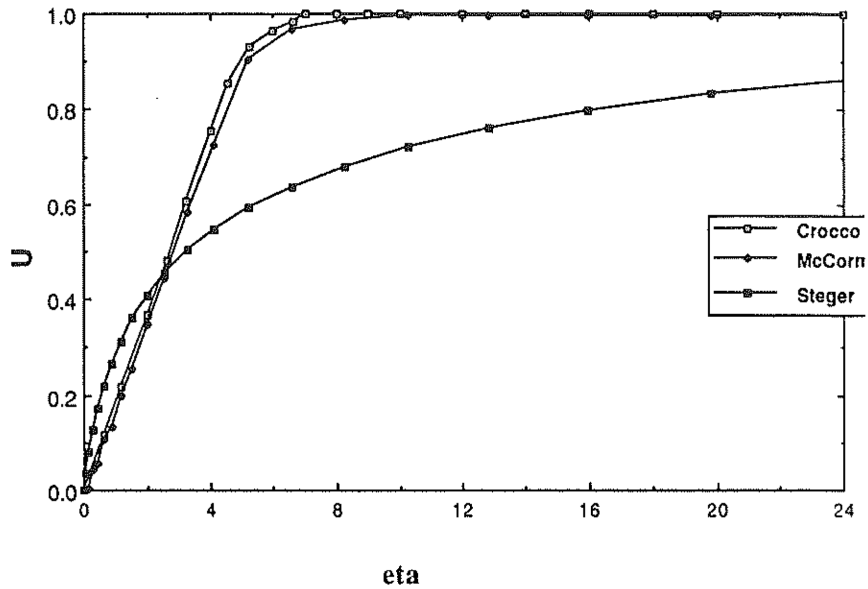

FIGURE 3. Velocity in boundary layer above flat plate at Mach = 2.

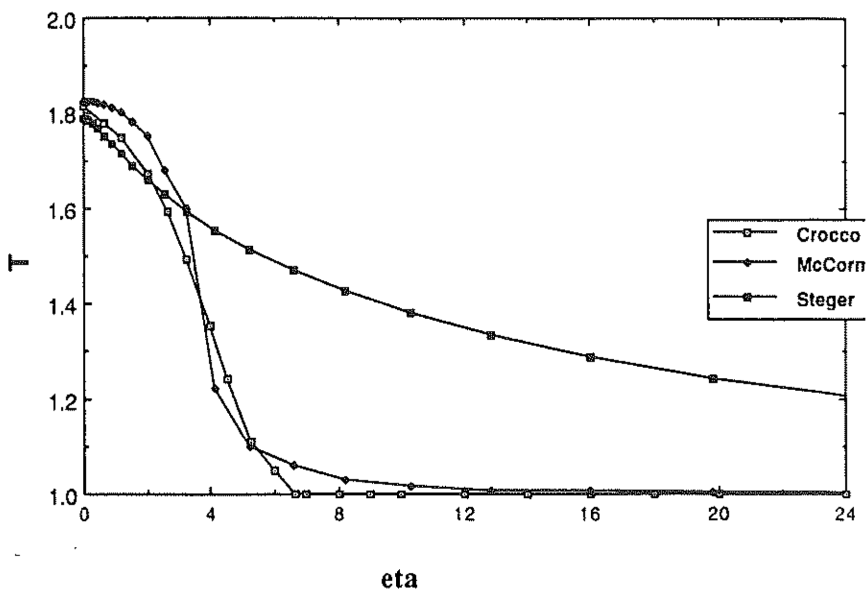

FIGURE 4. Temperature in boundary layer above flat plate at Mach = 2.